Magnetic Fields of Birkeland Currents

D. E. Scott, Ph.D. (EE)

Abstract: The fundamental vector calculus definition of a force-free, field-aligned, Birkeland current is expanded in cylindrical coordinates to obtain the partial differential equations (DEs) that yield the magnetic field created by such a current. The resulting equations are put into state-variable form and an Euler, step-wise, approximation incorporating a 4th order Runge-Kutta algorithm is applied. In single-variable form, the DEs are identified as Bessel equations. $J_0(r)$ and $J_1(r)$ Bessel function solutions confirm the Euler results thus yielding closed form solutions for both the linking (azimuthal) and collinear (axial) components of the force-free field. Results show that both of these magnetic components reverse their directions and vary in magnitude in a way that aids the formation of concentric cylindrical shells of matter as has been observed in Marklund convection. Another result is the finding that magnetic fields extend relatively farther from Birkeland currents than they would from a straight-line current. They slowly decay as $1/\sqrt{r}$ for large r.

Introduction

The entity that is often called a Birkeland current (and at other times a 'magnetic rope[i]' or 'vortex current') is most descriptively termed a 'field-aligned current'. This concept is usually counter-intuitive for anyone new to the study of electricity in the cosmos. Even those who are aware of the properties of electric and magnetic fields have usually only seen examples where electric fields and currents are at right angles (orthogonal) to magnetic fields. Electric motors and generators are prime examples. So is the study of how cyclotrons or mass-spectrometers function. Most, if not all of these phenomena, are based on the Lorentz force that operates on a moving charge within a magnetic field:

$$f = v \times B \tag{1}$$

The cross product of the moving charge's velocity vector and the magnetic field vector implies that the scalar value of the resulting force is given by

$$f = vB\sin\theta \tag{2}$$

where θ is the smallest angle between the vectors v and B. So if that angle becomes zero-valued, the force disappears.

Most examples of the interaction of electric currents and magnetic fields are presented in an earthbound context wherein the current is confined (and its direction thus controlled by) the shape and placement of the wire (or glass tube in the case of plasma) within which it exists. Current will flow wherever the wire is placed. If a motor is wired correctly, the Lorentz force will exist and the motor rotor will spin. This is not necessarily so in space. The conductors there are plasma. These plasmas are not confined and are able to move around and change their shape much more easily than can a wire stapled to a wall or cemented inside a motor housing.

Whenever things can move around, they tend to seek a minimum-energy configuration. "Water flows downhill." Objects tend to move in submission to applied forces – they move in such ways as to minimize the forces they experience.

In cosmic plasma, an electric current and its associated magnetic field are free to take on a minimum-energy configuration. This arrangement is described as a force-free field[ii] and has the property that:

$$(\nabla \times B) \times B = 0 \tag{3}$$

or

$$j \times B = 0 \tag{4}$$

The equivalence of expressions 3 and 4 is due to one of Maxwell's equations

$$\nabla \times B = \mu\left(j + \varepsilon \frac{\partial E}{\partial t} \right) \tag{5}$$

Therefore, assuming no time varying electric field is present, the Curl *B* vector will have the same direction as the current density vector, *j*. Both expressions (3 and 4) indicate that the magnetic field and the current that causes it will not push or pull on each other when they are exactly aligned. Such an arrangement is termed a *field-aligned current.* Expression 3 will be obeyed if the curl of *B* is proportional to *B* itself (if the current density, *j*, has the same direction as *B*). According to expression 3, this will occur if

$$\nabla \times B = \alpha B \tag{6}$$

where α is an arbitrary positive scalar quantity. If we are considering a Birkeland current, the natural coordinate system to use is, of course, cylindrical. (See figure 1.)

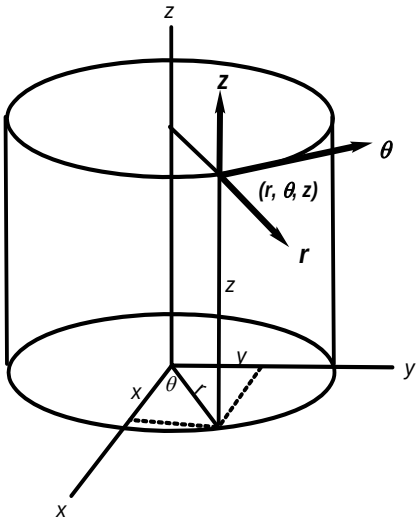

Figure 1. Cylindrical Coordinates

Expression 6 can be expanded in those cylindrical coordinates as follows:

$$\begin{aligned}\nabla \times B = &\left(\frac{1}{r}\frac{\partial B_z}{\partial \theta} - \frac{\partial B_\theta}{\partial z} \right) \boldsymbol{r_1} \\ &+ \left(\frac{\partial B_r}{\partial z} - \frac{\partial B_z}{\partial r} \right) \boldsymbol{\theta_1} \\ &+ \left(\frac{1}{r}\frac{\partial}{\partial r}(rB_\theta) - \frac{1}{r}\frac{\partial B_r}{\partial \theta} \right) \boldsymbol{z_1} \\ = \alpha B = &\ \alpha(B_r \boldsymbol{r_1} + B_\theta \boldsymbol{\theta_1} + B_z \boldsymbol{z_1})\end{aligned} \tag{7}$$

It is reasonable to expect no variation of the magnetic field as a function of the variables θ or *z*, therefore the first, second, third, and sixth partial derivatives in expression 7 are assumed to be zero-valued.

Thus we have:

$$\left(-\frac{\partial B_z}{\partial r} \right) \boldsymbol{\theta_1} + \left(\frac{1}{r}\frac{\partial}{\partial r}(rB_\theta) \right) \boldsymbol{z_1} = \alpha(B_\theta \boldsymbol{\theta_1} + B_z \boldsymbol{z_1}) \tag{8}$$

Separating similar vector components yields

$$\left(-\frac{\partial B_z}{\partial r} \right) = \alpha B_\theta \tag{9}$$

and

$$\left(\frac{1}{r}\frac{\partial}{\partial r}\left(rB_\theta\right)\right) = \alpha B_z \tag{10}$$

We are left with two coupled differential equations[iii] (9 and 10) in two dependent variables (B_θ, and B_z). The independent variable in both is r.

Euler Method of Solution

Because expression 10 is a differential equation (DE) containing a variable coefficient (one that depends on the independent variable) a closed-form solution is not easily obtained. Various methods have been developed for approximating the solution to such equations.[iv] Control engineers are occasionally confronted with non-stationary systems – ones where the coefficients in the describing differential equations vary with time[v]. In the system being investigated here, the independent variable is not time, but rather radial distance, r, measured outward from the central z-axis of the Birkeland current stream. The mathematical difficulties are, however, similar. Typically *state-variable analysis* is used in these cases.

A set of state variables for a system consists of the quantities that describe where (and how much) energy is stored in the system. A set of state equations is written with first derivatives of each state variable appearing on the left of the equal signs. No derivatives appear on the right sides of the equations – only state variables. In order to describe expressions (9) and (12) in state-variable form, the product rule for derivatives is applied to (10) as follows:

$$\frac{\partial\left(rB_\theta\right)}{\partial r} = r\alpha B_z \tag{11}$$

$$r\frac{\partial B_\theta}{\partial r} + B_\theta = r\alpha B_z \tag{12}$$

Since energy is stored in magnetic fields, state-variables may be defined as follows:

$$x_1 = B_z \tag{13}$$

$$x_2 = B_\theta \tag{14}$$

so that, rewriting expressions (9) and (12) in state-variable form yields

$$x_1' = -\alpha\, x_2 \tag{15}$$

and

$$x_2' = \alpha\, x_1 - 1/r\, x_2 \tag{16}$$

Using (15) and (16) an Euler (approximate, step-wise) solution of these equations was implemented. Conceptually, each state-variable defines the dimensional distance of a point in space relative to the origin. Derivatives (such as expressions 15 and 16) are thought of as being the velocities of the point along each of those dimensions. If the independent variable (usually time) is quantized in steps of h units, then multiplying each velocity (derivative expression) by h yields the incremental distance the point travels along any given axis during that small time interval. Finally, the value of each state-variable is updated by this incremental distance to get a new value of the variable (position of the point in state-space). A spreadsheet was used to obtain such an approximate solution. In order to improve accuracy, a fourth-order Runge-Kutta predictor-corrector algorithm was incorporated. In iterative solutions such as this, choosing the initial and incremental values for the discretized variables is as much an art as it is a science.

Results

The results, presented in figure 2, show the total magnetic field strength[vi] as being strongest at the minimum radial value (r = 1) and then decreasing with increasing r.

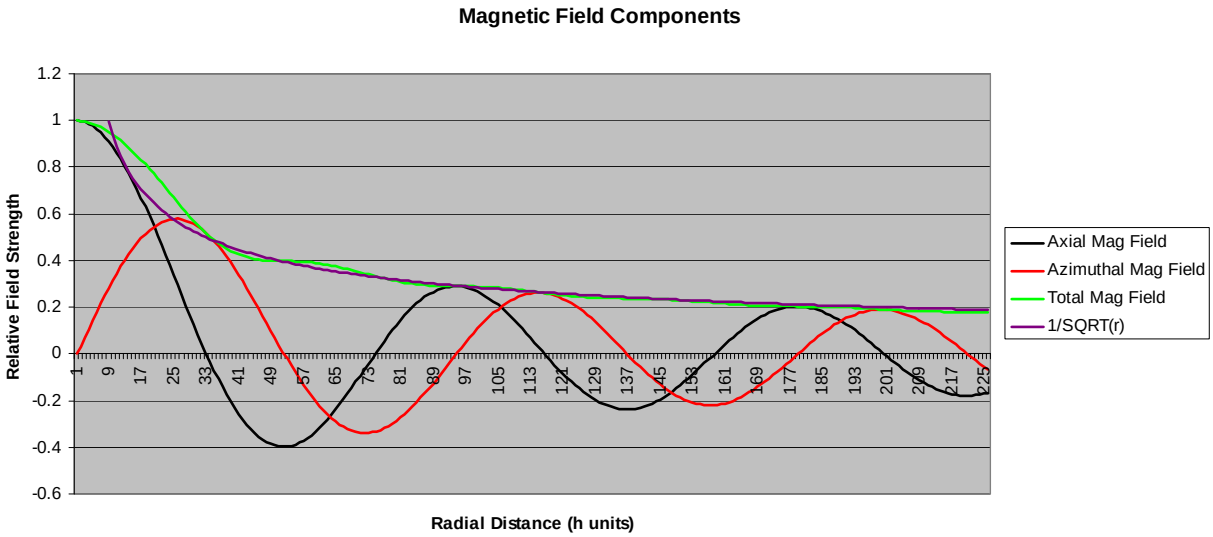

Figure 2. Magnitude of the axial (B_z), azimuthal (B_θ), components and the total (vector sum) magnetic field yielded by the Euler-RK algorithm.

Combining expressions 15 and 16 yields a single DE in a single dependent variable.

$$r^2 \frac{d^2 B_z}{dr^2} + r \frac{d B_z}{dr} + \alpha^2 r^2 B_z = 0 \tag{17}$$

Solution in Closed Form

A good friend of the author, Dr. Jeremy Dunning-Davies, recognized this DE as being one with which he was intimately familiar. He wrote saying, "I knew that resulting second order differential equation to which I referred rang a bell; it's almost identical to Bessel's equation of order zero – it just has the added factor of alpha squared in the non-differential term."

So, thanks to Dr. Dunning-Davies, we do indeed have closed-form solutions for the dependent variables in the DE that results from expanding equation (3). The solution to equation 17 is:

$$B_z = J_0(r) \tag{18}$$

$$= 1 - \frac{r^2}{2^2} + \frac{r^4}{2^2 4^2} - \frac{r^6}{2^2 4^2 6^2} + \ldots \tag{19}$$

This is the Bessel function of the first kind of order zero. The recursion relation for the next order function is

$$\frac{d J_0(r)}{dr} = -J_1(r) \tag{20}$$

Thus, from expressions 13, 14, and 15

$$B_\theta = J_1(r) \tag{21}$$

$$= \frac{r}{2} - \frac{r^3}{2^2 4} + \frac{r^5}{2^2 4^2 6} - \frac{r^7}{2^2 4^2 6^2 8} + \ldots \tag{22}$$

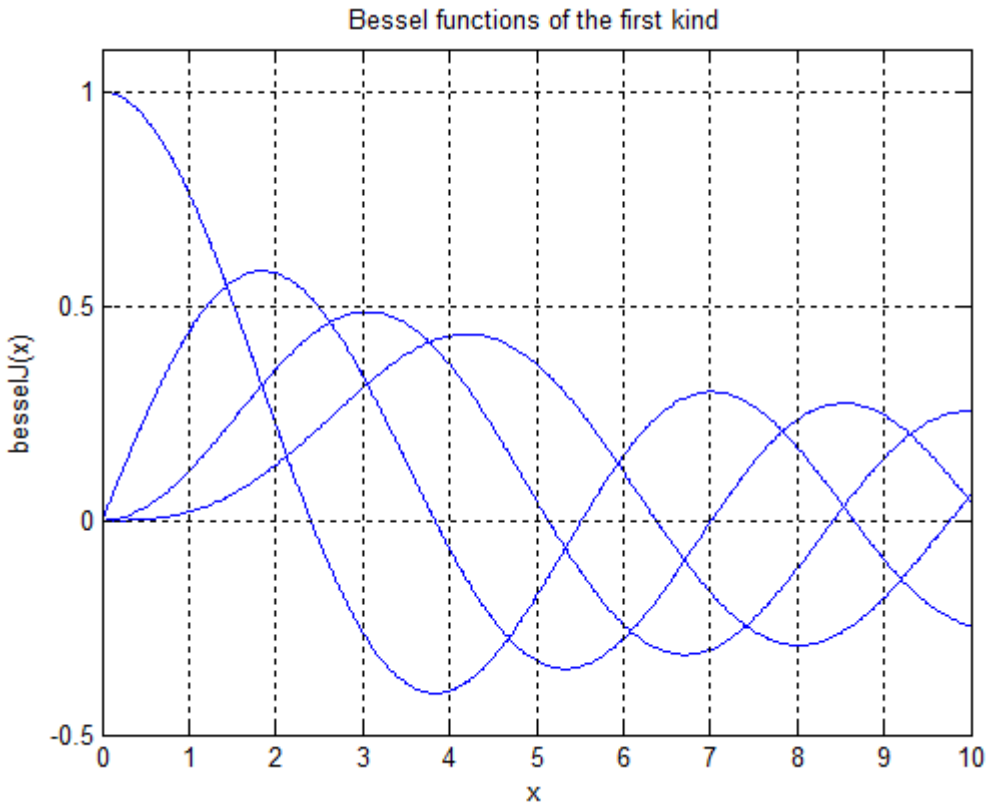

Figure 3. Bessel Functions[vii] of the first kind, J_0 through J_3 are closed-form solutions of equations 9 and 17.

These Bessel functions are sometimes called cylinder functions[viii] or cylindrical harmonics. We[ix] see that they are damped trigonometric functions for large x, but the amplitude decrease is very gradual. It goes as $1/\sqrt{x}$, which is much more gradual than exponential, $1/x$, or $1/x^2$ damping. The overall strength (amplitude) of the total magnetic field that surrounds a Birkeland current decreases with increasing radial distance from the axis of the current as shown in the third series in figure 2. The magnetic field strength decreases asymptotic with the $1/\sqrt{r}$ curve that is plotted there for reference. This is an unexpected result in that the magnetic field created by a long straight current decreases as $1/r$. Therefore, the magnetic fields of Birkeland currents extend outward in space much farther and less diminished in strength than the field that would be generated by a simple straight-line of electric current.

Consequences of the oscillatory nature of the solutions

Both these solutions (the Euler-RK approximation of figure 2 and the closed form Bessel functions in figure 3) are in one-to-one correspondence. They clearly show repeated reversals in the directions of both the axially directed and the azimuthal magnetic field components with increasing radial distance. This implies the existence of a continuum of concentric cylindrical surfaces wherein both the axially directed magnetic component, B_z, and the azimuthal component, B_θ, periodically change direction and decrease in strength with increasing radial distance out from the central z-axis. Where the magnitude of the axial field, B_z, is strongest, the azimuthal (encircling) field component, B_θ, goes through a zero-value as it reverses its direction of encirclement of the central current density vector, j. The axial and azimuthal field strengths are seen to be in quadrature relation with one another (it must be remembered that this is a

variation with changing outward distance, r – not time). For example in figure 2, in a region such as between radial distances 74 and 115, the axial field, B_z, is unidirectional (in the positive z-direction, with maximum strength at ~ r = 94). The azimuthal field reverses direction at r = 94, changing from the negative theta direction to positive. This results in a total magnetic field vector that rotates (with increasing r) in a clockwise direction as we view it when looking down a radius toward the axis of the current. The alternating direction of the azimuthal magnetic field component, by itself, may aid the layering effect noted in the Marklund[x] convection process in Birkeland currents in space. Marklund states, "The filamentary structures are analyzed as helical twisted magnetic flux tubes where the magnetic field is approximately force free. Under the influence of electric and magnetic fields the ionized component of the plasma will drift inward,…"

The analysis presented here assumes that the axial direction, z, is by definition the direction of the current density, j, of the Birkeland current. We make no assumption that the direction of that current does not change over long distances – only that, whatever direction j takes on, z is collinear with it. So the current density, j, is everywhere collinear with the z-axis. Therefore, as Marklund correctly states, the Lorentz force will be inward, toward the axis, wherever B_θ is positive. For example, from figure 1, it is seen that a proton (+charged mass) traveling in the z-direction and moving through a region of positive-valued B_θ, will experience an inwardly directed Lorentz force, $F_L = v_p \times B_\theta$. Electrons traveling in the negative z direction will similarly be forced inward, toward the z-axis. However, where a +ion moving in the +z direction passes through a region of negatively directed B_θ, the force will be outward.

Continuing this same line of thought, (remembering that matter will tend to be thrust outward in regions of negative B_θ) and with reference to figure 2, consider points (radial distances) such as r = 94, or r = 178. At these values of r, the B_θ component is transitioning from negative to positive. Therefore, below each of these radii, matter will be pushed upward, away from the z-axis and, above those points, matter will be pushed downward. Thus material will be pushed into concentric cylindrical shells (as is observed in the Marklund convection process). This concentrated matter ought to be found in cylindrical shells whose radii coincide with alternating zeros of the $B_\theta = J_1(r)$ Bessel function. These surfaces are located[xi] at r = 7.0156, 13.3237, 19.6159, …in figure 3.

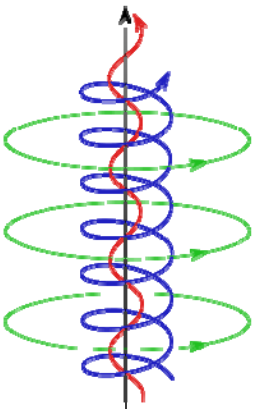

We note the Alfvén image[xii] (figure 4), that is used to describe the Birkeland Current magnetic field, is in agreement with these results (but only for small r). As r increases beyond what is shown in figure 4, a continuous increase of the pitch angle of the magnetic helixes occurs as described above. This increase does not stop at 90°. The axis of a Birkeland current is wrapped with a compound helical magnetic field whose pitch increases continuously with increasing radial distance. This gives rise to a structure suggestive of Roman fasces. It is perhaps analogous to wrapping a pipe with tape. The first layer of applied tape is laid on in parallel strips that do not go around the pipe at all. The second layer has a very gentle pitch, only completing one encirclement in a large distance down the pipe. Increasing layers have progressively sharper pitches, until one layer makes no progress along the

Figure 4. Schematic drawing showing the pitch angle of the magnetic field as a function of *r*.

pipe – only encircling it. This analogy is a dangerous one if carried too far: there are no discrete layers in the magnetic field structure – it is a continuum. The pitch angle of the helical field increases smoothly (continuously), and unboundedly, with increasing radius. This property is shown schematically in figure 5.

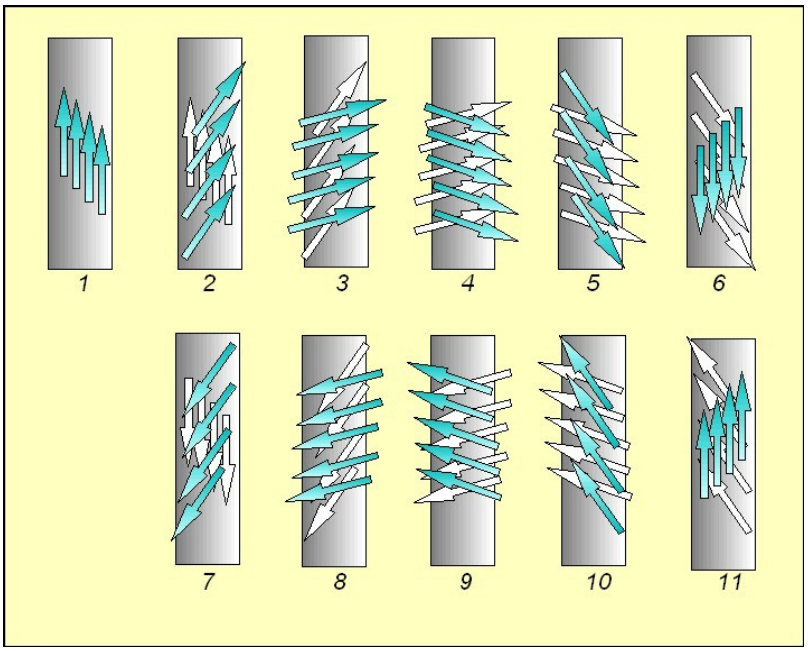

Figure 5. The pitch angle of the helical total vector-magnetic field that encircles a Birkeland current increases continuously with increasing radial distance. There are no quantum jumps in the pitch angle nor in the field's amplitude. In this figure, one cycle (0°-360°) of the pitch angle is shown. The cycle is sketched at eleven sample increasing radius values. The light blue arrows show the total magnetic field direction at each value of radius, *r*, while the white arrows show the field direction just below that (at *r – dr*).

The qualitative properties of the plots in figure 2 and their implications are listed in table 1.

J_n zeros	Radii Fig. 2	Effect, B_θ value	B_z value	Helix pitch angle	Description: viewer sees
0	0	Matter layer, Bth =0	*Bz max +z*	0	Matter headed away
2.4	33	F in = max, Bth = +max	*Bz =0*	90	Bth clockwise
3.83	51	Matter rare, Bth=0	*Bz max –z*	180	Nothing
5.5	74	F out = max, Bth= -max	*Bz=0*	270	Bth counter-clockwise
7.02	94	Matter layer, Bth=0	*Bz max +z*	360 = 0	Matter headed away
8.7	116	F in = max, Bth= +max	*Bz=0*	90	Bth clockwise
10.17	136	Matter rare, Bth=0	*Bz = -max*	180	Nothing
11.8	158	F out = max, Bth = -max	*Bz=0*	270	Bth counter-clockwise
13.32	178	Matter layer, Bth=0	*Bz = +max*	360 = 0	Matter headed away
14.9	199	F in = max, Bth = +max	*Bz = 0*	90	Bth clockwise
16.47	220	Matter rare, Bth =0	*Bz = -max*	180	Nothing

Table 1. Summary of the properties of a Birkeland current's magnetic field as a function of radius, *r*.

The fifth column of table 1 indicates several radial values where the helical pitch angle is either zero or 180°. At those points, true force-free current can theoretically exist parallel to the z-axis.

However we note that the 180° (anti-parallel) radii are locations where the Lorentz force sweeps matter away to both higher and lower radial values. Thus, the number of available charge carriers in those particular regions is few to none. It is as if a high-speed highway were built there, but there are no cars present that want to use it.

The right-hand column of table 1 indicates what a viewer would see looking "up the gun-barrel" (in the positive *z*-direction) of a Birkeland current in the same direction as the receding current density vector, *j*. This is shown graphically in figure 6.

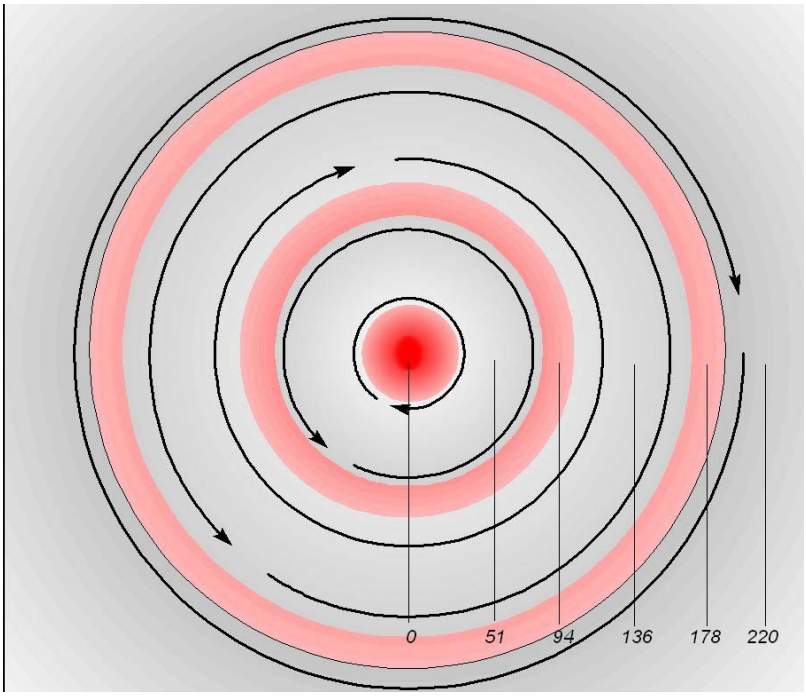

Figure 6. Cross-section view of a Birkeland current. Matter concentrations shown in red/pink.

The radius values in figure 6 correspond to those in figure 2 and in column 2 of table 1. The directions of the azimuthal magnetic field, B_θ, at various radii are also shown. At these particular radial values, the axial field, B_z, is zero valued and so B_θ constitutes the total field. It is clear that in regions surrounded by positive (clockwise) B_θ, charged matter is compressed inwardly toward the *z*-axis by the Lorentz force. In regions above – at greater radial values than negatively directed (counter-clockwise) B_θ, matter is pushed outward by that same mechanism. In this way, the three concentration regions at r = 0, 94, and 178 are formed. Similarly the evacuated regions around radii = 51, 136, and 220 result from the same process. The concentrations are shown in red in figure 6. They consist of charged particles that can carry current. Thus these hollow cylindrical shells are the likeliest regions to be visible, if any are, in a given Birkeland current. For example, images such as figures 7, and 10 below, have been obtained in plasma laboratories, and figures 8, and 9 in actual astronomical observations.

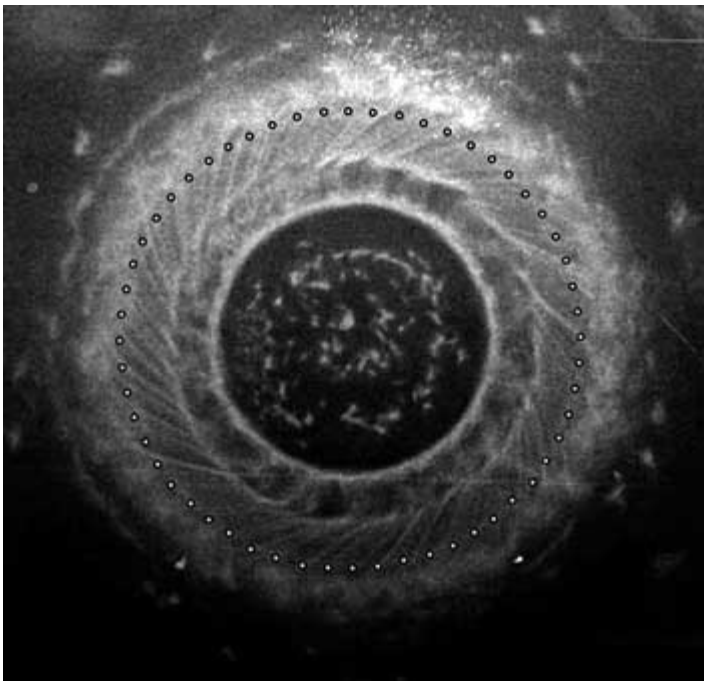

Figure 7. Penumbra of a dense plasma focus from a discharge current of 174,000 amperes. — Credit A. L. Peratt.

Figure 8 clearly shows the concentric cylindrical structure of a well-known planetary nebula[xiii].

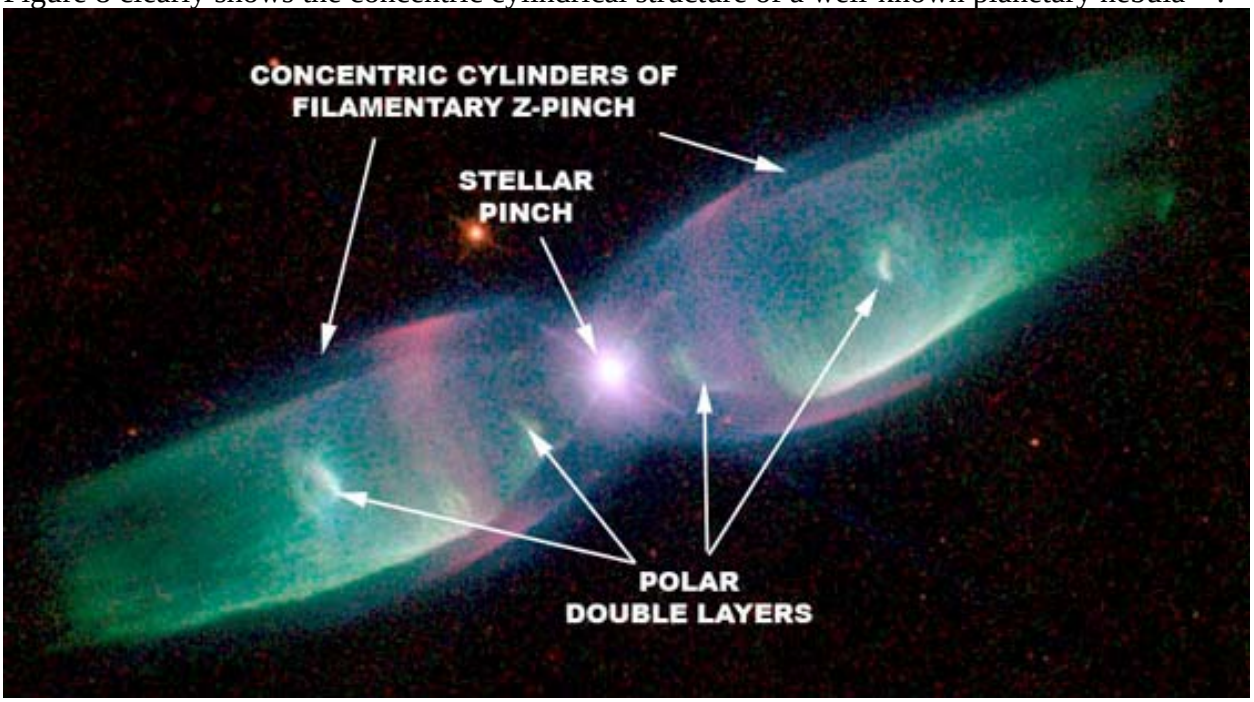

Figure 8. An inter-stellar Birkeland current *z*-pinch. The double concentric cylindrical structure is obvious in this image on both sides of the central pinch.

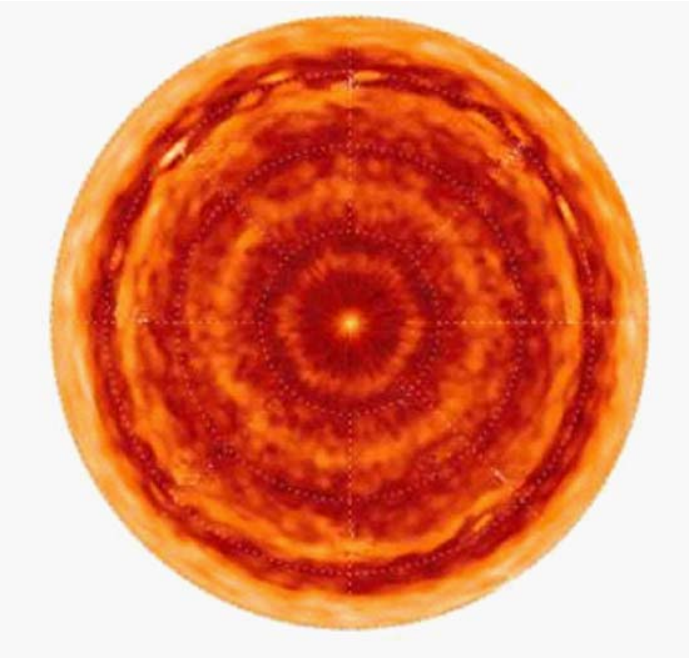

The image shown in figure 9 is consistent with the hypothesis that Saturn is receiving a flow of electrical charge via a Birkeland current directed into its poles. This image appears in, and is discussed by Stephen Smith in the TPOD of May 28, 2013 entitled *Saturn's Northern Hotspot*[xiv].

Figure 9. The north pole region of Saturn – Infrared image. **Credit NASA/JPL/Oxford University.**

Matter that becomes radially stratified is primarily ionized. However neutral dust can also be carried along in the process.

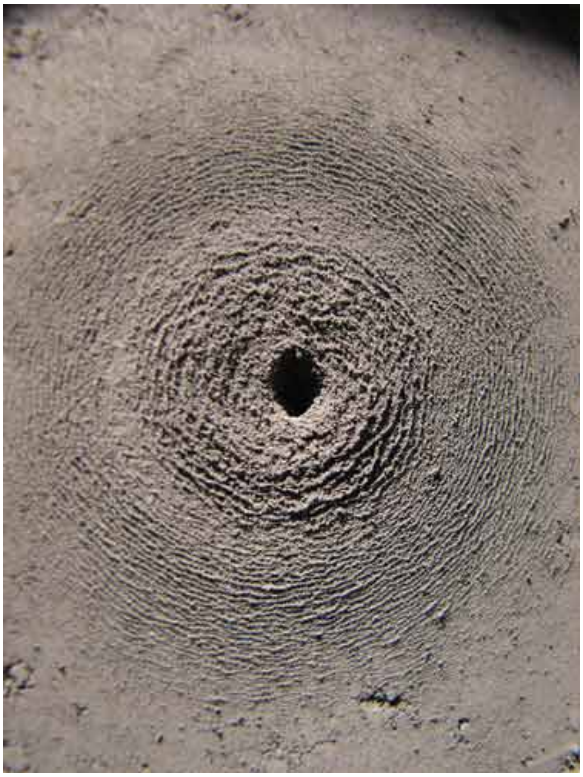

Figure 10. Laboratory result of an electric plasma discharge in air. **Credit: Vemasat Labs**

Unconstrained electric discharges in air are just as capable of forming force-free configurations as those in space. Dr. C. J. Ransom and Mel Acheson at Vemasat Laboratories obtained the radial pattern shown in figure 10 via a 10 second (μA level) electric discharge into an earthlike material (manganese peroxide).

Conclusions

The major conclusion that can be taken from this work is – the definition of a "field-aligned" (force-free) current dictates that the overall controlling differential equation that identifies the shape and strength of the magnetic fields surrounding Birkeland currents is the Bessel equation. This single fact produces three secondary findings:

1. These magnetic fields stretch out much farther, and with greater potential effect, than previously thought. For large radial distances, the amplitude of those fields varies (slowly decays) as $1/\sqrt{r}$.
2. The helical structure of those fields is more complicated than previously thought. The angle of pitch of the helix increases smoothly and continuously with increasing radial distance, *r*, from the axis of the current.

3. The Lorentz force that results from the varying strength and alternating direction of the azimuthal field component (with increasing *r*) produces concentric cylinders of concentrated matter that surround the axis of the current. These layers are separated by regions from which matter is swept away (both upward and downward) toward the neighboring regions of high matter concentration. This ionized matter constitutes a set of concentric, hollow, cylindrical, conducting paths.

A Final Point

This analysis has been an exercise in identifying the spatial differential equation that results from following the basic, defining vector calculus definition of field-aligned Birkeland currents (expression 3) to its logical conclusions. That defining expression seems intuitive and reasonably based. After accepting its validity, and making certain simplifying assumptions, the derivation is purely mathematical. As is always the case in such derivations, whether the assumed model accurately describes the actual physical situation is a question. Any predicted properties such as oscillations may be artifacts – aberrations due solely to method that are not in the real-world physical process. As this author has previously stated repeatedly, mathematics ought to be a guide from which astrophysics can take direction for future investigations. Confirming experimental observations are the touchstone by which the validity of mathematical derivations such as these must be judged – not the other way around.

Acknowledgement

The author wishes to express sincere thanks to Dr. Jeremy Dunning-Davies for recognizing the single variable differential equation as being that of Bessel, and identifying the solutions.

DES July 2013

Endnotes and References

[i] Eastwood, J., *Flux ropes*, NASA, Godard Space Flight Center, Greenbelt, MD., 2009. THEMIS discovered a flux rope pumping a 650,000 Amp current into the Arctic.
[ii] Peratt, A. L., *Physics of the Plasma Universe*, Springer-Verlag 1992, p. 28. Available: http://link.springer.com/book/10.1007/978-1-4612-2780-9.
[iii] At this point ordinary derivatives could be used, however because the variables can have time-dependence, partial derivatives are used for clarity of purpose.
[iv] Bellman, R.E.,et al, *Identification of Differential Systems with Time-Varying Coefficients*, Rand Corp. Available: http://www.rand.org/pubs/research_memoranda/RM4288.html
[v] Bartels, R.E., *A Numerical Scheme for ODEs Having Time Varying and Nonlinear Coefficients Based on the State Transition Matrix*. NASA, Langley research Center, Hampton, VA. Available: http://www.ingelec.uns.edu.ar/asnl/Materiales/Cap05Extras/SLLVT/NASA-2002-tm211776.pdf
[vi] Computed as the square root of the sum of the squares of the two component fields, B_z and B_θ.
[vii] Available: http://www.mathworks.com/help/symbolic/besselj.html
[viii] Bessel Functions of the First Kind, *Wolfram MathWorld*. Available: http://mathworld.wolfram.com/BesselFunctionoftheFirstKind.html
[ix] ME 201…Bessel Functions, Available: http://www.me.rochester.edu/courses/ME201/webexamp/bessfunc.pdf
[x] Marklund, G.T., *Plasma convection in force-free magnetic fields as a mechanism for chemical separation in cosmical plasmas*, *Nature* **277**, 370 - 371 (01 February 1979) Available: http://www.nature.com/nature/journal/v277/n5695/abs/277370b0.html

[xi] Harrison. J., *Fast and Accurate Bessel Function Computation*, Intel Corp., Available: http://www.cl.cam.ac.uk/~jrh13/slides/arith-09jun09/slides.pdf
[xii] Alfvén, Hannes *Evolution of the Solar System*. Washington. D.C., USA: Scientific and Technical Information Office, National Aeronautics and Space Administration (1976).
[xiii] Planetary Nebula "HourGlass", M2-9[xiii] Available: http://www.thunderbolts.info/wp/2013/05/27/saturns-northern-hot-spot-2/ See also http://www.nasa.gov/mission_pages/cassini/multimedia/saturn_hotspot-cap20080103.html

DONALD E. SCOTT - CURRICULUM VITAE

The author earned his Bachelor's and Master's degrees from the University of Connecticut, Storrs, and his Ph.D. degree from the Worcester Polytechnic Institute, Worcester, MA, all in electrical engineering.

He was with General Electric (Large Steam Turbine Generators) in Schenectady, NY, and Pittsfield, MA (Lightning Arrester Division).

From 1959 to 1998, he was a member of the faculty of the Department of Electrical and Computer Engineering, University of Massachusetts, Amherst. He was, at various times, an Instructor, Assistant Professor, Associate Professor, Assistant Department Head, the Director of the undergraduate program, Graduate Admissions Coordinator, and Director of the College of Engineering's Video Instructional Program.
In 1984, he was a Guest Lecturer in the School of Engineering, University of Puerto Rico, Mayaguez. Dr. Scott was the recipient of several good-teaching awards during his thirty-nine years on the faculty of UMass, Amherst.

He is the author of:
A 730 page text: *An Introduction To Circuit Analysis—A Systems Approach* (McGraw-Hill Book Company, 1987,) and
The Electric Sky—A Challenge to the Myths of Modern Astronomy (Mikamar Publishing, 2006). This second book addresses the legitimacy of many of the assumptions, hypothetical entities, and forces that are required by presently accepted non-electrical, gravity-only-based theories in astrophysics.

He is the author of several technical papers in the area of electric circuits and systems design.

In 2009 he presented an invited seminar on Plasma Cosmology to engineers, astronomers, and astrophysicists at NASA's Goddard Space Center, Greenbelt, MD. Some of his recent papers, reports, lectures and images are accessible below:

Solar Electron Flux - New Discovery 2013
Voyager I Data Confirms ES Model
Interview of Scott About New Data
Astronomical Images by Scott
Solar Surface Transistor Action
Properties of EM Fields and Plasma in the Cosmos (IEEE paper)